12C.4 UPPER TROPOSPHERIC TEMPERATURE IMPACTS ON IDEALIZED HURRICANES

Benjamin C. Trabing* and Michael M. Bell
Department of Atmospheric Sciences, Colorado State University, Fort Collins, CO

1. Introduction

The temperature of the tropical tropopause layer (TTL) has found to be important for our understanding of the potential intensity (PI) a tropical cyclone (TC) can attain (Emanuel 1986; Emanuel et al. 2013). TCs can be equated to Carnot heat engines (Emanuel 1986, 1997, 2003) where an increase in the outflow temperature results in a reduction of the amount of work a TC could have otherwise used to power the winds against frictional dissipation.

Past studies have examined the role that changing tropopause temperatures will have on PI in radiative convective equilibrium (RCE). Wang et al. (2014) found that the PI for TCs in RCE increased with cooler tropopause temperatures. Ramsay (2013) analyzed the effects of lower stratospheric cooling finding that TCs in RCE had a higher PI due to an increase in thermal efficiency. These studies have shown that upper tropospheric temperatures can modulate TC intensity over long timescales but have not diagnosed the physical mechanisms by which this happens on weather timescales. Both Ramsay (2013) and Wang et al. (2014) used fixed radiative profiles which prevented radiative feedbacks within the TCs. It is not well understood how radiation may interact with the TTL temperatures to modify PI.

Using idealized high-resolution simulations, this study examines how varying upper tropospheric temperature profiles and radiation impacts TC intensity to diagnose possible mechanisms behind these differences.

2. Methods

Due to the complicated interactions between clouds, radiation, and storm dynamics, we resort to idealized simulations. The Weather Research and Forecasting (WRF) model version 3.7.1 (Skamrock et al. 2008) is employed.

Environmental soundings were derived from temperature observations from the National Centers for Environmental Prediction Climate Forecast System Reanalysis. Monthly temperature products were averaged to create mean soundings for 10N, 20N, and 30N with tropopause temperatures of 196.3K, 199.9K, and 202.9K respectively. These three thermodynamic profiles were then averaged below 200hPa.

Due to model sensitivities an ensemble approach was taken. For each sounding, 15 ensemble members were simulated by introducing random mixing-ratio perturbations between ±.5g kg^{-1} to the lowest pressure level (Van Sang et al. 2008). The simulations will herein be referred to by their tropopause temperatures (i.e. TT196, TT199, TT202).

Each simulation had two-way nested doubly-periodic domains with 18, 6, and 2km resolution. Experiments were conducted on an aquaplanet with fixed sea surface temperatures at 301K with an F-plane approximation ($F=.5\times10^{-5}$ s^{-1}). Simulations

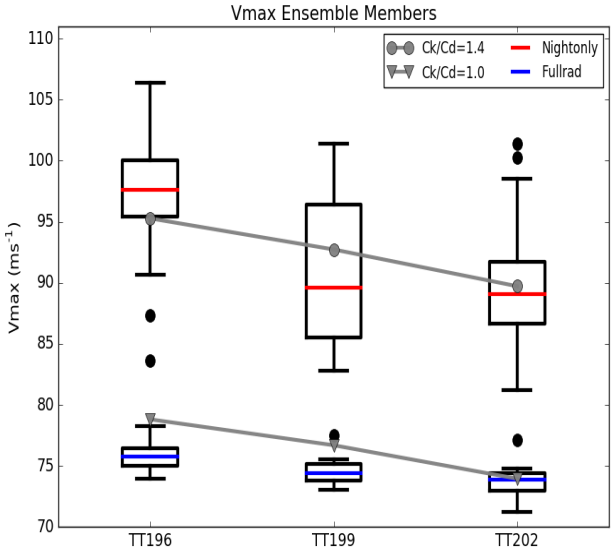

Figure 1. Boxplot of V_{max} for each ensemble member for the Nightonly (red) and Fullrad (blue) simulations. The 25th and 75th interval is indicated by the box with outliers in filled black circles where the distance between the box was greater than 1.5 times the width of the box. Gray lines are the theorized PI (Bister and Emanuel 1998) using different relationships between the ratio of exchange coefficients.

* *Corresponding author address*: Benjamin C. Trabing, Colorado State University, Department of Atmospheric Sciences, Fort Collins, CO 80526; email: Btrabing@colostate.edu

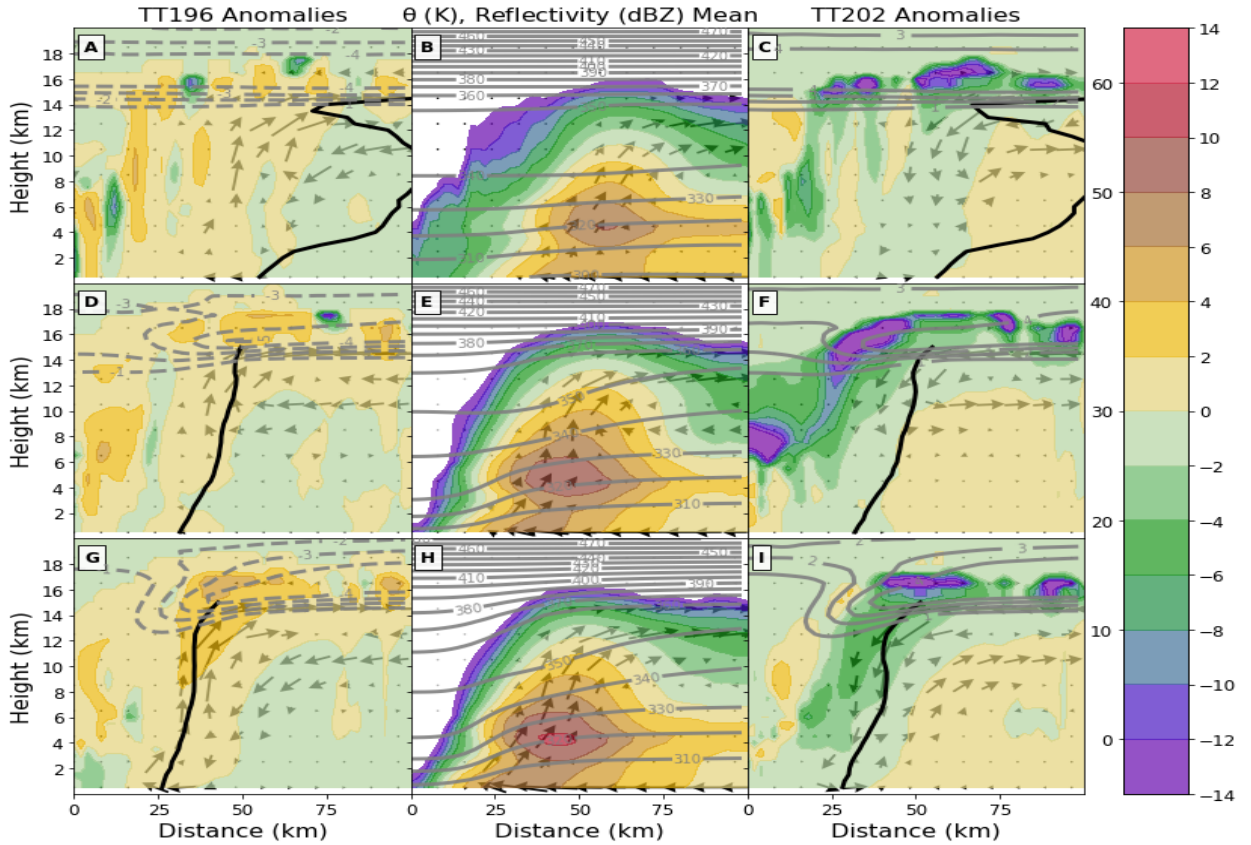

Figure 2. Axisymmetric mean potential temperature (θ, contoured) and reflectivity (shaded) for Nightonly simulations between t=24-48h (A, B, C), t=48-72h (D, E, F), and t=72-96h (G, H, I). Middle panel plots (B, E, H) are the ensemble means with θ contours every 10K and reflectivity shaded every 5 dBZ with reflectivity below -5 dBZ whited out. Left paneled plots (A, D, G) show the anomalies of TT196 from the ensemble mean and right paneled plots (C, F, I) show the anomalies of TT202. The θ anomaly contour interval is 1K and the zero line has been removed for clarity. Negative θ anomalies are dashed. Black line indicates RMW up to 15km. Secondary circulation denoted by wind vectors with magnitudes less than 1 m s^{-1} removed. The wind vectors have been increased by a factor of five in the vertical only.

were performed using the Thompson aerosol-aware microphysics scheme (Thompson and Eidhammer 2014), the Yonsei University planetary boundary layer scheme (Hong et al. 2006), New Tiedtke convective parameterization (Tiedtke 1989) on the outer domain, and was initialized with a weak vortex (Rotunno and Emanuel 1987). The Rapid Radiative Transfer Model (Mlawer et al. 1997) was used for longwave radiation with the Dudhia scheme for shortwave radiation (Dudhia 1989).

Two sets of experiments were conducted using the derived thermodynamic profiles. One experiment includes both shortwave and longwave radiation and will be referred to as Fullrad. The second experiment includes turning off the shortwave heating and will be referred to as Nightonly. This results in a total of six experiments and allows us to analyze radiative feedbacks not present in past studies that employed RCE.

3. Results

The variability of V_{max} and how our simulations compared to PI theory are shown in Figure 1. The Nightonly simulations were sensitive to the boundary layer moisture perturbations while the Fullrad simulations were not. By adjusting the ratio of the non-dimensional surface exchange coefficient for enthalpy and the drag coefficient (C_k/C_D) we get similar ensemble V_{max} and PI values. The relationship between V_{max} and upper tropospheric temperatures appears linear with colder temperatures causing stronger TCs on average.

Although differences in ensemble means exist between the Fullrad and Nightonly experiments, the anomalies are qualitatively similar. In Figure 2, TT202 has lower reflectivity values above the eyewall and along the inner edge of the eyewall while TT196 has more. This is indicative of a

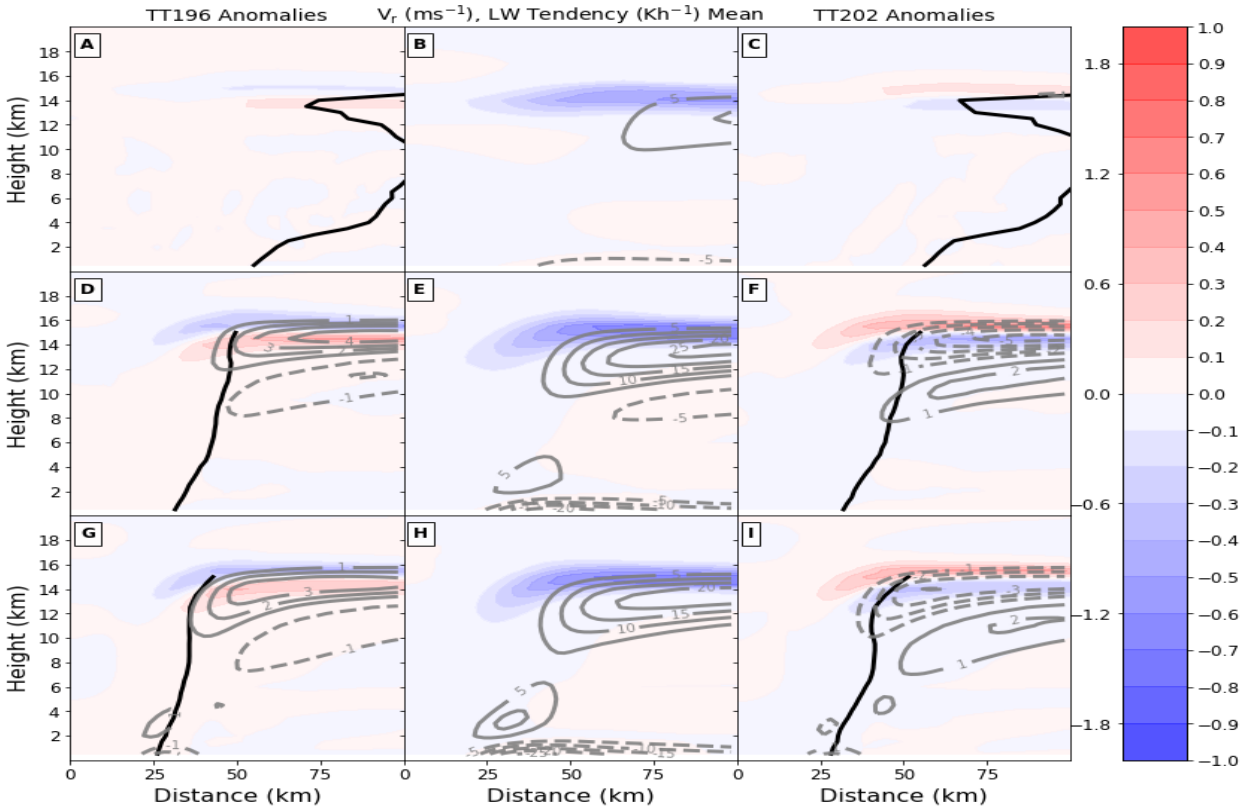

Figure 3. Axisymmetric mean radial wind (contoured) and net radiative tendencies (shaded) for Nightonly simulations between t=24-48h (A, B, C), t=48-72h (D, E, F), and t=72-96h (G, H, I). Middle panel plots (B, E, H) are the ensemble means with radial wind contour intervals of 5 m s^{-1}. Left paneled plots (A, D, G) show the anomalies of TT196 from the ensemble mean and right paneled plots (C, F, I) show the anomalies of TT202. The radial wind contour interval is 1 m s^{-1} with the zero line removed from each plot for clarity. Negative radial winds are dashed. Black line indicates RMW up to 15km.

change in height of the clouds and therefore more ice aloft in TT196. In the potential temperature fields, the initial temperature modifications persist but get reduced above the eye with time as the warm core strengthens. The secondary circulation anomalies show an anomalous toroidal circulation that is first located at the upper levels prior to influencing surface winds. This means that TT196 had stronger vertical motion in the eye and stronger outflow.

Longwave heating tendencies (Figure 3) for the Nightonly simulations strengthen as the TC strengthens with a dipole developing outside the radius of maximum winds (RMW). In TT196 we have a cooling anomaly over a warming anomaly and vice versa for TT202. This anomaly is again due to the cloud tops of the TCs being at different levels. The vertical gradient in heating corresponds to the development of the outflow anomalies which is the expected response from the Eliassen model (Eliassen 1952). Although TT196 TCs are stronger and have locally increased longwave cooling, there is less integrated cooling such that the Carnot heat sink is actually reduced.

4. Conclusions

The ensemble means agree with PI theory that the cooling of upper tropospheric temperatures will cause an increase in V_{max} and a warming will result in reduced V_{max}. However, the magnitude of this relationship and its linearity is sensitive to radiation in addition to small boundary layer moisture perturbations.

The ensembles showed that upper tropospheric temperatures and radiation played an important role in changing the dynamic and thermodynamic structure of the TCs. Colder TTL temperatures resulted in deeper TCs with more reflectivity at higher levels while warmer upper tropospheric temperatures yielded the opposite. These heating anomalies in the radiative tendencies caused the response in the secondary circulation expected from the Eliassen equation. This effect was

sensitive to the radiation as the Nightonly simulations caused, stronger heating anomalies, stronger anomalies in the secondary circulation, and overall stronger TCs compared to the Fullrad simulations. The results of this study further suggest that cloud-radiative feedbacks have a non-negligible impact on weather timescales and improvements are necessary to our understanding of radiation in the Carnot cycle model.

6. References

Bister, M., and K.A. Emanuel, 1998: Dissipative heating and hurricane intensity. *Meteor. Atm. Phys*., **52**, 233-240.

Dudhia, J., 1989: Numerical Study of convection observed during the Winter Monsoon Experiment using a mesoscale two dimensional model. *J. Atmos. Sci.,* **46,** 3077-3107.

Eliassen, A. (1952), Slow thermally or frictionally controlled meridional circulations in a circular vortex, *Astrophys. Norv.*, **5**, 19–60.

Emanuel, K.A., 1986: An air-sea interaction theory for tropical cyclones. Part I: Steady state maintenance. *J. Atmos. Sci*., **43**, 585-604.

Emanuel, K.A., 1997: Some aspects of hurricane inner-core dynamics and energetics. *J. Atmos. Sci*., **54**, 1014-1026.

Emanuel, K., 2003: Tropical Cyclones. *Ann Rev. Earth Planet. Sci*., **31**, 75-104.

Emanuel, K., S. Solomon, D. Folini, S. Davis, and C. Cagnazzo, 2013: Influence of tropical tropopause layer cooling on Atlantic hurricane activity, *J. Clim*., **26**(7), 2288–2301.

Hong, S.-Y., Y. Noh, and J. Dudhia, 2006: A new vertical diffusion package with an explicit treatment of entrainment processes. *Mon. Wea. Rev.*, **134**, 2318–2341.

Mlawer, E. J., S. J. Taubman, P. D. Brown, M. J. Iacono, and S. A. Clough, 1997: Radiative transfer for inhomogeneous atmospheres: RRTM, a validated correlated-k model for the longwave. *J. Geophys. Res.,* **102**, 16 663-16 682.

Ramsay, H. A., 2013: The effects of imposed stratospheric cooling on the maximum intensity of tropical cyclones in axisymmetric radiative–convective equilibrium. *J. Climate,* **26**, 9977–9985.

Rotunno R, Emanuel KA. 1987. An air-sea interaction theory for tropical cyclones. Part II: Evolutionary study using a nonhydrostatic axisymmetric numerical model. *J. Atmos. Sci.* **44**: 542 – 561.

Skamarock, W. C., and Coauthors, 2008: A description of the Advanced Research WRF version 3. NCAR Tech. Note NCAR/TN-475+STR, 113 pp.

Thompson, G., and T. Eidhammer, 2014: A study of aerosol impacts on clouds and precipitation development in a large winter cyclone. *J. Atmos. Sci.*, **71**, 3636–3658.

Tiedtke, M., 1989: A comprehensive mass flux scheme for cumulus parameterization in large-scale models. *Mon. Wea. Rev*, **117**, 1779–1800.

Van Sang, N., R. K. Smith, and M. T. Montgomery, 2008: Tropical cyclone intensification and predictability in three dimensions. *Quart. J. Roy. Soc.*, **134**, 563-582.

Wang, S., S. J. Camargo, A. H. Sobel, and L. M. Polvani, 2014: Impact of the Tropopause Temperature on the Intensity of Tropical Cyclones: An Idealized Study Using a Mesoscale Model. *J. Atmos. Sci.,* **71**, 4333-4348.